Glioblastoma targeting via integrins is concentration dependent

ARTICLE *in* BIOTECHNOLOGY AND BIOENGINEERING · OCTOBER 2009

Impact Factor: 4.13 · DOI: 10.1002/bit.22424 · Source: PubMed

3 AUTHORS, INCLUDING:

Elena V Rosca
University of Hull
18 PUBLICATIONS **253** CITATIONS
SEE PROFILE

Robert Gillies
Moffitt Cancer Center
353 PUBLICATIONS **14,521** CITATIONS
SEE PROFILE

ARTICLE

BIOTECHNOLOGY and BIOENGINEERING

Glioblastoma Targeting Via Integrins Is Concentration Dependent

Elena V. Rosca,[1,2] Robert J. Gillies,[3] Michael R. Caplan[1,2]

[1]Harrington Department of Bioengineering, Arizona State University, PO Box 879709, Tempe, Arizona 85287-9709; telephone: 480-965-5144; fax: 480-727-7624; e-mail: michael.caplan@asu.edu

[2]Center for Interventional Biomaterials, Arizona State University, Tempe, Arizona

[3]Department of Radiology, University of Arizona, Tucson, Arizona

Received 29 January 2009; revision received 14 May 2009; accepted 22 May 2009

Published online 1 June 2009 in Wiley InterScience (www.interscience.wiley.com). DOI 10.1002/bit.22424

ABSTRACT: A novel approach to treat cancer more selectively is achieved by targeting drugs to cells via conjugating the drug or imaging agent to an antibody or ligand for a cell surface receptor that is over-expressed by the target cell population. Previous work by us has suggested that enhanced specificity can be obtained by multivalency of binding moieties. In this study we investigated the binding specificity of a multivalent construct including three peptides segments (TWYKIAFQRNRK), which bind the $\alpha_6\beta_1$-integrin, linked by poly(ethylene glycol) spacers. The binding specificity of the constructs was calculated by quantifying their binding to target cells (glioma cells, SF 767) relative to non-targeted cells (normal human astrocytes, NHA). Dodecapeptide constructs (monovalent) exhibit specificity equal to the ratio of receptor expression at all concentrations. However, trivalent constructs demonstrated a sharp increase in specificity at concentrations less than the affinity of the receptor–ligand bond (4.28 μM). These experiments (conducted at 4°C) were consistent with the theoretical prediction and indicate that the biophysical model captures the basic trend of the data in the absence of receptor internalization, although the concentration at which increased specificity is observed is greater than predicted. The biophysical model does not predict the results of 37°C experiments, and this is shown to be due to internalization which occurs at 37°C but not at 4°C.

Biotechnol. Bioeng. 2009;104: 408–417.

KEYWORDS: drug delivery; cell surface receptor; glioblastoma; protein-binding; macromolecular substance

Introduction

Drugs or imaging molecules are typically administered systemically and act upon their target based on characteristics of those target cells (e.g., increased metabolism or increased cell division). The major drawback of this approach is that the drugs also affect non-targeted cell populations leading to side effects and limiting safe dosages which results in limited efficacy toward the target cells. A novel approach to circumvent this problem is targeting drugs to cells by conjugating the drug or imaging agent to an antibody or ligand for a cell surface receptor that is over-expressed by the target cell population (Balthasar et al., 2005).

Biophysical modeling predicts that this strategy will increase the local concentration near target cells relative to the local concentration near non-target cells (Caplan and Rosca, 2005; Rosca et al., 2007). If that can be achieved, it would either allow decreasing overall dose to achieve the same efficacy with fewer side effects or maintaining the overall dose to achieve greater efficacy (greater local concentration) toward the target cells while maintaining the known side effects. One example of this strategy, by Madhankumar et al., describes the targeting of high grade brain tumors such as gliomas by employing nanospheres modified with sterically stable human interleukin-13 capable of binding the over-expressed IL-13 receptor on the glioma cells. Doxorubicin was loaded into IL-13-conjugated liposomes, and this method of delivery resulted in enhanced cytotoxicity to glioma cells due to greater internalization compared to free drug and non-target cells (Madhankumar et al., 2006).

If antibodies or ligands are conjugated to imaging contrast agents or fluorophores, they can be used as diagnostic tools as well. Imaging molecules conjugated to VEGF fragments or VEGF antibodies, matrix metalloprotease inhibitors, E-selectin binding peptide, endoglin (CD105)

Correspondence to: M.R. Caplan
Contract grant sponsor: NIH
Contract grant number: R21 NS051310; K22 DE014386
Contract grant sponsor: Arizona Biomedical Research Commission
Contract grant number: 0606

antibodies and Arg-Gly-Asp (RGD) have been used to detect or localize inflammation or cancer (Cai et al., 2006). Depending on the imaging agent conjugated, these can be used in positron emission tomography (PET) or single-photon emission computed tomography (SPECT) imaging (VEGFR, radiolabled RGD or MMPs), while others have been used in magnetic resonance imaging (MRI) and ultrasound (integrin directed nanoparticles) (Cai et al., 2006). A study by Rosenthal et al. (2007) investigated labeled anti-EGFR antibodies to delineate tumor edge, and it concluded that such intra-operative labeling approaches increase the efficacy of total tumor resections.

Several investigators have proposed conjugating multiple antibodies or ligands to enhance the ratio of binding to target versus non-target cells (which we define as "specificity") via cooperativity. Caplan and Rosca (2005) predicted that such an approach could indeed increase specificity above the ratio of receptors on target versus non-target cells; however, this improvement is predicted to occur only at construct concentrations less than the affinity of the receptor–ligand bond. If this hypothesis is valid, it would suggest a trade-off between specificity (achieved at low concentration) and intensity of imaging or efficacy of therapy (achieved at high concentration). Since antibodies are characterized by very strong binding affinities (nanomolar), achieving increased specificity through multiple antibodies would only be possible at picomolar concentrations (Caplan and Rosca, 2005; Carlson et al., 2007).

While several studies have demonstrated that multivalent constructs achieve increases in avidity (Handl et al., 2004; Ye et al., 2006), few studies have measured true specificity. The distinction is necessary because it is possible to make constructs more avid without making them more specific. For example, if a construct becomes more avid for the target cells but becomes just as much more avid for the non-target cells, specificity will be unchanged. Lowery et al. (2006) compared the binding of nanoparticles to cancer cells and non-cancerous cells through imaging and then through thermal ablation. The particles were found to have preferentially bound to the cancer cells. Rosca et al. (2007) also studied polymeric constructs and found that there were qualitative differences in binding to glioblastoma cells versus normal astrocytes. However, neither of these studies quantified the ratio of local concentrations nor did they test the hypothesis that concentration of the construct is a critical parameter to achieving this specificity.

In this study we investigate the binding specificity of polymeric, multivalent constructs targeted to the $\alpha_6\beta_1$-integrin (shown schematically in Fig. 1). The specificity is investigated by quantifying binding of fluorescently labeled, multivalent constructs to target cells (glioma cells, SF 767) and non-targeted cells (normal human astrocytes, NHA). The multivalent construct incorporates three dodecameric peptides (TWYKIAFQRNRK) whose sequence was discovered and characterized by Nakahara et al. (1996). The peptide is derived from the globular domain of the laminin α_1 chain and inhibits cell adhesion to laminin-1 (90% inhibition). The same study also demonstrated that the peptides interacts mainly via the $\alpha_6\beta_1$-integrin by receptor neutralization studies by showing that adhesion to the peptide-coated substratum was 80% inhibited by an anti-α_6 antibody (compared to minimal inhibition by antibodies to other α-subunits. The $\alpha_6\beta_1$-integrin is targeted because it is known to be over-expressed in migratory glioma cells (Gingras et al., 1995) and occupying these integrins with targeting constructs may have the added benefit of hindering cell migration.

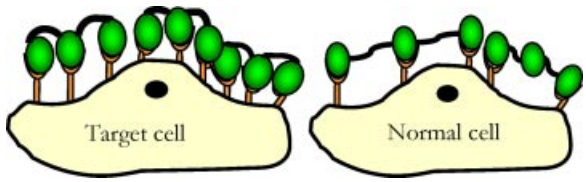

Figure 1. Schematic representation of binding of multivalent constructs to target and non-target cells. The number of constructs on the target cells is greater than the number of constructs on the non-target cell leading to greater therapeutic concentration near the target cells or greater intensity of imaging contrast agent near the target cells. [Color figure can be seen in the online version of this article, available at www.interscience.wiley.com.]

This study tests the hypothesis that multivalent constructs exhibit greater specificity in comparison to dodecameric peptides only at concentrations of constructs less than the affinity of the receptor–ligand bond. We also compare the quantitative value of specificity achieved to predictions made using a mathematical model of the biophysics of construct–cell interactions.

Material and Methods

Synthesis of Constructs

Constructs were synthesized using standard solid phase chemistry. The protocol was described in detail in Rosca et al. (2007). Briefly, the trivalent construct consists of three dodecapeptides (TWYKIAFQRNRK) connected by two linkers which are each constructed of three units of Fmoc-NH-$(PEG)_2$-COOH (20 atoms, *N*α-Fmoc-19-amino-5-oxo-3,10,13,16-tetraoxa-6-azanonadecan-1-oic acid, Novabiochem, Gibbstown, NJ) to form a peptide-linker-peptide-linker-peptide structure. At the amine end of the construct a molecule of fluorescein isothiocyanate (FITC, Anaspec #20151) or biotin (Anaspec, Freemont, CA) is added according to the manufacturer protocol. The constructs are cleaved from the resin, purified using standard protocols, and verified by MALDI-TOF. The monovalent construct consists of one dodecapeptide with a FITC molecule added to the amine end of the construct.

Binding Assays

Normal human astrocytes (NHA) and glioma cells (SF767) were generously supplied by Michael Berens (Translational Genomic Institute, Phoenix, AZ). Cells were maintained under standard conditions (37°C and 5% CO_2) and were grown in Dulbecco's modified Eagle medium (DMEM) supplemented with 10% bovine growth serum (BGS). Cells were plated on coverslips (22 mm × 22 mm) in 6-well plates, coated with 0.1% gelatin, at a density of 250,000 cells per well the day prior to experiments. On the day of the experiments, cells were incubated with binding media (DMEM, 1 mM 1,10-phenanthroline, 200 mg/L bacitracin, 0.5 mg/L leupeptin, and 3% BSA, 0.01% Tween 20) for 30 min at 4°C (Fig. 2) or 37°C (Figs. 4 and 5) to block non-specific binding. The constructs were diluted in binding media (dilutions from 20 to 0.6 μM) and incubated with the cells at 4°C (Fig. 2) or 37°C (Figs. 4 and 5) for 1 h with gentle rocking. Counterstaining of the nuclei was performed using 4′,6-diamidino-2-phenylindole (DAPI) (3 μg/mL). Following incubation, cells were washed 4 times with wash buffer (50 mM Tris–HCl, 30 mM NaCl, and 0.5% BSA) and incubated with PBS containing Ca^{2+} and Mg^{2+} (100 mg/L).

Images were acquired using Zeiss Axiovert 200M inverted microscope equipped with AxioCam MRm camera, on each sample. Four random fields were imaged per sample. Each image was adjusted in Adobe Photoshop (version 5.0.2) using the curve adjustment feature which allowed the development of a standard curve that was used on all the images for each corresponding construct and concentration. To quantify the images, the phase contrast image was used to choose a representative cell per field, the area of this cell was delineated, that area was mapped onto the fluorescence image for the same field, and the fluorescence intensity in that area was calculated. Three measurements per image were performed, and specificity was calculated by taking the ratio the intensity of fluorescence for the two cell types. Each experiment was performed in duplicate. An average specificity measurement per pair of images was obtained, and *t*-tests ($P < 0.05$) between multivalent and dodecapeptide at each concentration were performed to establish statistical significance. DAPI staining provided an internal control.

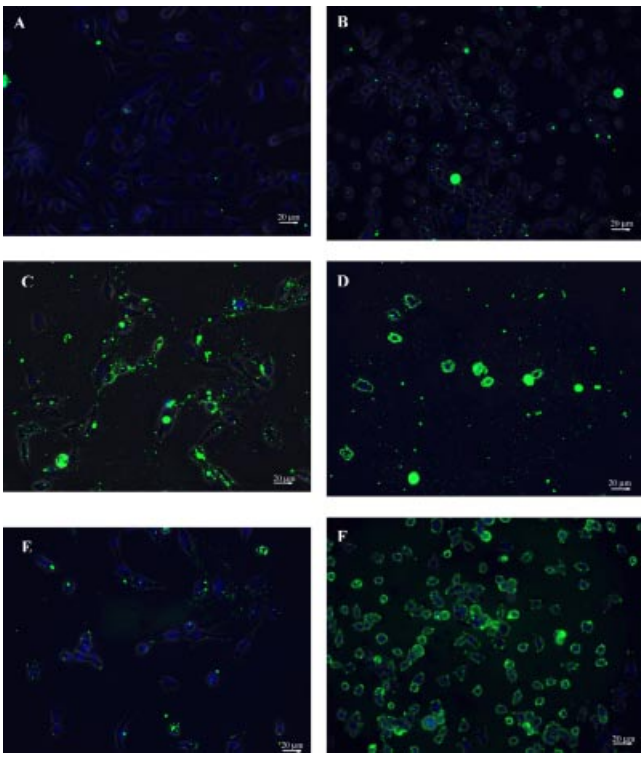

Figure 2. Epifluorescence images of constructs bound to astrocyte cells (NHA) and glioma cells (SF767). **Panels A** (NHA) and **B** (SF767) illustrate minimal binding of the dodecameric construct to both cell types at 10 μM. At the same concentration (10 μM) the trivalent construct exhibits intense binding on both cell types, **panels C** (NHA) and **D** (SF767). At 0.625 μM, the trivalent construct exhibits minimal binding on the NHA cells (**panel E**) but maintains intense binding on the SF767 cells (**panel F**).

Flow Cytometry

Expression of $\alpha_6\beta_1$-integrin on the two cell types was quantified using flow cytometry. Cells were harvested using PBS/EDTA (7 mM EDTA) and incubated in DMEM with 1% BSA. Cells were incubated with Phycoerythin (PE) conjugated antibodies for the α_6 subunit (BD Biosciences, #555736) for 1 h with gentle rocking at 4°C. Following labeling, cells were washed 3 times with DMEM containing 1% BSA. Fluorescence was quantified using BD FACSCalibur. Receptor number was calibrated to fluorescence intensity using BD QuantiBRITE PE bead kit. A sample of PE labeled beads is run immediately following the experimental samples, using the same instrument settings. According to the manufacturer specification a standard curve for the fluorescence intensity and number of fluorophores per bead is constructed and used to calculate the number of receptors per cell assuming a one to one binding ratio (one PE-antibody per cellular integrin).

Western Analysis

Western blot analysis was performed on whole cell extracts and pull down assay of cell extracts using biotinylated trivalent constructs coupled to streptavidin beads. Cell extracts were prepared by harvesting the cells with PBS/EDTA mixture and incubating the cell pellet with lysis buffer (50 mM Tris, 150 mM NaCl, 1% Triton, 100 μL/mL protease inhibitors cocktail, Sigma, St. Louis, MO, #P8340) for 2 h at 4°C with gentle rocking. The biotinylated construct (1 mg of construct per 1 mL of bead solution) was coupled

with Sepharose Streptavidin coated beads (GE, Piscataway, NJ, # 17-5113-01) in binding buffer (10 mM Tris, 2 M NaCl, 1 mM EDTA) at 4°C with gentle rocking for 1 h. The washed beads were incubated with cell extract (normalized for the amount of protein, based on bicinchoninic acid protein assay) for 1 h at 4°C. The pull down was dissociated by boiling the beads in SDS loading buffer for 10 min. A negative control was performed by incubating cell extract (same amount of protein) with beads alone without the biotinylated construct. The samples were separated by SDS–PAGE (6%) and transferred to PVDF membrane for antibody probing. After blocking 1–2 h with blocking buffer at 4°C (Licor, Lincoln, NE, #927-40000), the blot was incubated with anti-α_6 antibodies (Santa Cruz, Santa Cruz, CA, #sc-6597) overnight at 4°C. After 3-4 washes, the blot was developed with secondary IR-dye antibodies (Licor, #827-08364) and the blot was read using Odyssey Infrared imaging system. The scan was analyzed with the Odyssey software.

Mathematical Modeling

A mathematical model of multivalent targeting by Caplan and Rosca (2005) is made non-dimensional using the length, time, and concentration scales as in Stukel et al. (2008). These result in an equation for the dimensionless concentration of unbound construct, $\hat{L}$, and dimensionless unbound receptor concentration, $\hat{R}$, which can be solved iteratively for $\hat{R}$ if $\hat{L}$ is assumed to be constant (sufficient pool of ligand):

$$-6V_R^2\hat{L}\alpha^3\hat{R}^3 - 12\alpha^2 V_R\hat{L}\hat{R}^2 - (6\alpha\hat{L}+2)\hat{R} + 2\delta = 0$$

where α is a non-dimensional parameter equal to R_0/K_D, K_D has units of [# cell^{-1}], R_0 is the number of receptors on the target cell, δ is the ratio of receptor expression between the cell type being calculated and the expression of the target cell, and V_R represents the binding enhancement factor for the multivalent construct as described by Shewmake et al. (2008). Equations for constructs bound by one ($\hat{C}_1$), two ($\hat{C}_2$), or three ($\hat{C}_3$) ligands are:

$$\hat{C}_1 = 3\alpha\hat{L}\hat{R}, \qquad \hat{C}_2 = \frac{\delta - (3\alpha\hat{L}+1)\hat{R}}{2+\alpha V_R\hat{R}},$$

$$\hat{C}_3 = \frac{\delta - (3\alpha\hat{L}+1)\hat{R}}{(6/\alpha V_R\hat{R})+3}$$

The non-dimensional equations for the non-target cells are identical to these except that δ equals 1 for the target cell but equals $R_{0,\text{non-target}}/R_{0,\text{target}}$ for non-target cells. Specificity is calculated as the ratio of total bound constructs (sum of all complexes on a cell type) on target cells versus non-target cells. The fit of the data in Figure 3A was determined by minimization of the square of the sum of errors for V_R while holding α and δ at measured values, 1.42×10^{-4} and 0.36, respectively. Other parameter values used are described in Results Section.

Results

Binding and Specificity at 4°C

FITC-labeled constructs were allowed to bind to SF767s or NHAs, and the ratio of intensity of binding between SF767s and NHAs is used as a relative measure of specificity. It has been demonstrated that receptor internalization is temperature dependent and that this process is arrested at 4°C (Gaietta et al., 1994). In order to study the biophysics of construct binding without confounding this with internalization kinetics, these experiments were performed at 4°C. Experiments at 37°C are described below. The effect of valence can be seen by comparing dodecameric peptide versus trivalent construct at identical concentration (10 μM) binding to NHAs (Fig. 2A vs. C) or to SF767s (Fig. 2B vs. D). In Figure 2A and B there is evident DAPI staining of nuclei but very little FITC indicating that binding between dodecameric peptide and cells is minimal at 10 μM. On the contrary, trivalent constructs at the same concentration bind in high quantity as demonstrated by the intense FITC staining in Figure 2C and D.

Specificity, however, is not determined by comparisons between monovalent and multivalent. Instead specificity is determined by comparison between multivalent binding to the target cells (SF767) and non-target cells (NHA). In comparing Figure 2C with D, there appears to be little difference in intensity and, when quantified, the ratio of fluorescence intensity is slightly greater than twofold. Although it is difficult to determine by eye, the ratio of fluorescence intensity between Figure 2A and B (dodecameric peptide) is also approximately twofold; thus, there is no advantage to multivalency at 10 μM construct. When concentration is decreased to 0.625 μM construct, binding to the NHAs is greatly reduced (Fig. 2E); however, binding to the SF767s remains high (Fig. 2F). The ratio of these fluorescence intensities is approximately ninefold. These data are quantified by calculating the ratio of fluorescence per cell (fluorescence intensity of one SF767 cell divided by fluorescence intensity of one NHA cell) and plotted as a function of construct concentration as shown in Figure 3A (circles are trivalent constructs, squares are dodecameric peptides). Dodecameric peptides at all concentrations show similar ratio of fluorescence as that between Figure 2A and B.

Mathematical Modeling

In previous work by Caplan and Rosca (2005) it was predicted that specificity in multivalent targeting would be a strong function of construct concentration and that increased specificity due to multivalency would only be observed at concentrations less than the affinity of the receptor–ligand bond. In Figure 3A specificity data are compared to results from the mathematical model in which two of the three dimensionless parameters, dimensionless affinity (α) and

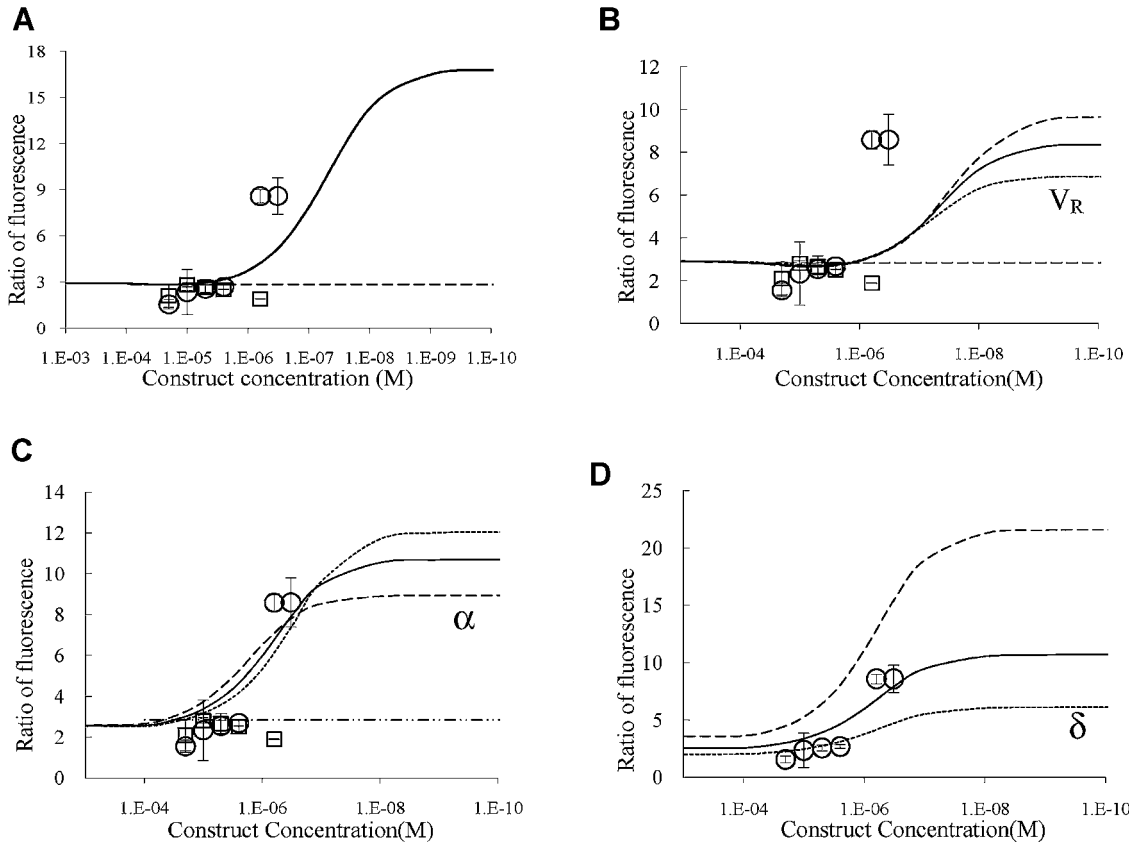

Figure 3. Ratio of fluorescence as a measure of binding specificity of trivalent construct (circles) and dodecapeptide (squares). **A**: Continuous lines depict theoretical binding specificity of the trivalent construct (solid line) and monovalent construct (dashed line) fit for V_R. Error bars depict 95% confidence intervals. **B**: V_R is set so that the plateau of maximal specificity equals the specificity of the measured value at the lowest concentration. Sensitivity analysis for V_R is included—increased (long dash) or decreased (short dash) by 30%. **C**: Sensitivity analysis for α as it was increased (long dash) or decreased (short dash) to the bounds of the 95% confidence interval of the measured values and best fit to data (thick solid). **D**: Sensitivity analysis for δ (over-expression ratio) as it was increased (long dash) or decreased (short dash) to the bounds of the 95% confidence interval of the measured values.

the ratio of receptor expression (δ), are set to experimentally measured values, 1.42×10^4 (Rosca et al., 2007) and 0.36, respectively, and the third parameter, V_R, is fit by minimizing the sum of the squares of the error to a value of 1.72×10^4. Experimental values to compare with these models were obtained by incubating either fluorescently labeled multivalent constructs or fluorescently labeled dodecapeptides with glioma cells and astrocytes at six different concentrations. The ratio of fluorescence intensity between glioma cells and astrocytes for the same construct and concentration is plotted in Figure 3; for example, intensity of fluorescence of trivalent construct at 0.625 μM incubated with glioma cells is divided by intensity of fluorescence of trivalent construct at 0.625 μM incubated with astrocytes to make the data point (circle) at 6.25×10^{-7} M and specificity equal to 8.58. Figure 3A shows that the data matches the model prediction that specificity is only enhanced at lower concentration; however, the model predicts that the transition to enhanced specificity will occur at a concentration lower than the actual value and that the specificity will be enhanced much more than it is in actuality. The latter may be an artifact of the least-squares fitting attempting to optimize the fit for the concentration at which the increase in binding affinity occurs. If the data points corresponding to the lowest concentration are assumed to represent a plateau and V_R is set to achieve a model result that plateaus at the same value of specificity (Fig. 3B), the result is a more realistic value of V_R (6.76×10^3) but the concentration at which specificity is enhanced is still predicted to be less than the observed transition concentration.

Based on the parameter values used to generate the curve in Figure 3B, sensitivity analysis of the three model parameters (V_R, α, and δ) is performed and shown in Figure 3B–D, respectively. V_R affects steepness of the increase in specificity as concentration decreases and also affects the magnitude of the enhancement of specificity. α affects both the magnitude of the enhancement of specificity as well as the concentration at which the transition to enhanced specificity occurs (weaker affinity moves the transition to greater concentration). Figure 3C shows a curve created by least-squares fitting both V_R and α

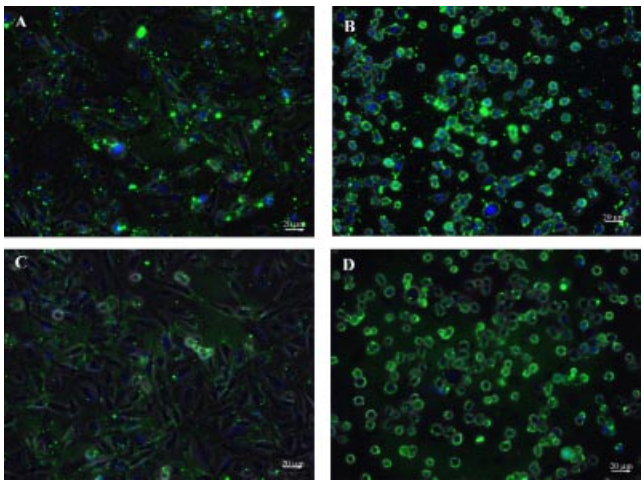

Figure 4. Epifluorescence images of trivalent constructs bound at 37°C. Constructs at 10 μM incubated with NHAs (**A**) or SF767 cells (**B**) and constructs at 0.625 μM incubated with NHAs (**C**) or SF767 cells (**D**) all exhibit intense fluorescence.

(1.7×10^6) to the data, and this value of α corresponds to an affinity of 1.9×10^{-4} M. This value of affinity is approximately two orders-of-magnitude weaker than the experimentally measured value $(4.28 \times 10^{-6}$ M) which suggests two likely possibilities. First, incorporation of the linear peptide sequences could have decreased its affinity by two orders-of-magnitude by sterically limiting its accessibility and conformational mobility. Second, this could indicate that the equations themselves are not including a biophysical phenomenon important to the function of these constructs. Finally, sensitivity analysis was performed on the ratio of receptor expression, δ, which primarily influences the magnitude of specificity enhancement by increasing or decreasing the value to which specificity plateaus at low concentration.

Binding and Specificity at 37°C

Although the biophysical model seems, with the possible exception of the concentration at which the transition to enhanced specificity occurs, to capture the behavior of these constructs at 4°C, it does not capture construct function at 37°C. When experiments were performed at 37°C, qualitative differences in fluorescence were observed between the SF767s and NHAs; however, no statistical differences in intensity were observed. Figure 4 shows trivalent constructs at two concentrations (10 and 0.625 μM) binding to cells at 37°C. In comparison to the binding at 4°C, fluorescence is much more intense on both cell types at 37°C, and the concentration dependence is much less pronounced.

In an effort to understand why the biophysical model does not match the results at 37°C, we performed an experiment in which cells are treated with trypsin to degrade any extracellular proteins or peptides. Figure 5 illustrates the results after trypsin treatment showing that both NHAs (Fig. 5A) and SF767s (Fig. 5B) retain the fluorescence even after trypsin treatment indicating that the construct is likely intracellular (integrin-bound constructs would most likely

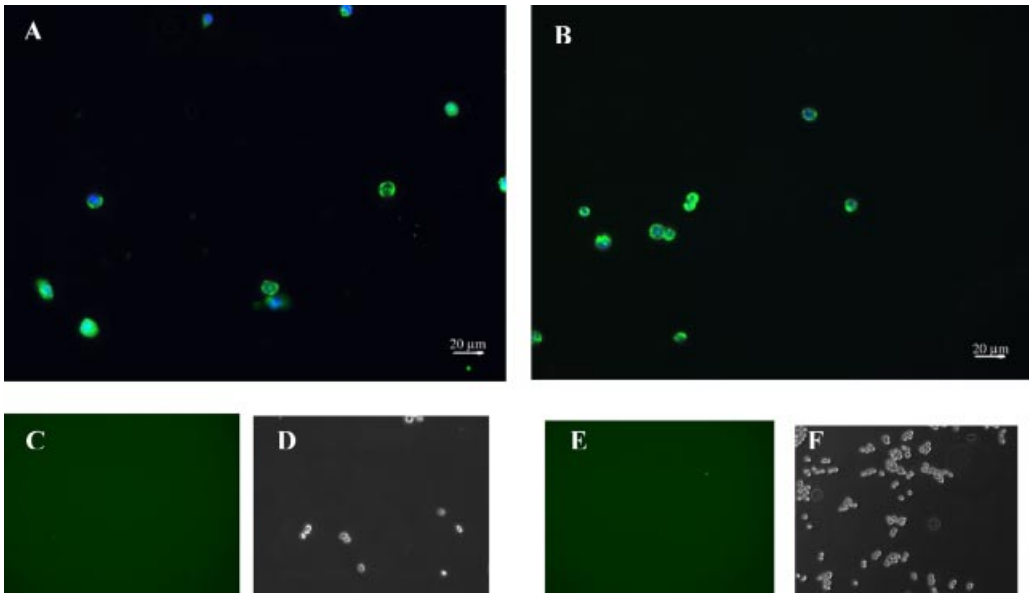

Figure 5. Epifluorescence imaging of cells labeled with the trivalent construct (0.625 μM) incubated at 37°C followed by trypsin treatment. After treatment with trypsin, NHA (**panel A**) and SF 767 cells (**panel B**) demonstrate persistent fluorescence indicating internalization of the construct. **Panels C–E** (C and D correspond NHA while E and F correspond to SF 767) depict epifluorescence and phase imaging of cells treated with the trivalent construct (0.625 μM) incubated at 4°C followed by trypsin treatment. No binding is visible on the cells after trypsin treatment.

have become unbound as trypsin degrades the integrins). Control cells, cultured at 4°C and treated otherwise identically, do not maintain fluorescence after trypsin treatment as shown by cells being visible in phase contrast (Fig. 5D and F) but with no discernable fluorescence above background (Fig. 5C and E). This suggests that all constructs were extracellular at 4°C matching expectation because cell internalization machinery does not function at 4°C (Gaietta et al., 1994). Although there are other possibilities to account for this difference, the major variation is the internalization ability; therefore, this is the most likely cause of this phenomenon.

Specificity Is Mediated Via α_6-Integrin Over-Expression

Since the ratio of receptor expression on SF767s versus NHAs should be a major parameter (δ) determining the specificity, we sought to quantify the expression of $\alpha_6\beta_1$-integrins on these cells by FACS. Antibodies for either the α_6 subunit or the β_1 subunit were available. Of these we used the α_6 because it is only known to form heterodimers (fully assembled integrin) with the β_1 and β_4 subunits; whereas, the β_1 subunit is known to form heterodimers with many α subunits. The expression of β_4 subunits was quantified and found not to vary between SF767 cells and NHA cells (data not shown) so differences in α_6 subunit expression should represent differences in $\alpha_6\beta_1$-integrin expression. α_6 expression by the SF767 cells is $37{,}600 \pm 270$, and expression by NHAs is $13{,}210 \pm 340$ integrins per cell. This results in a ratio of expression of 2.84 ± 0.07. This value is used as the parameter δ^{-1} in the model results shown in Figure 3 and compares well with the specificity observed for the monovalent constructs (2.39 ± 0.17) which should always equal this ratio of expression. Even though the two values 2.39 ± 0.17 and 2.84 ± 0.07 are statistically different in an unequal variance t-test ($P < 0.01$), they are similar; and the difference is somewhat expected since the measurements are the result of two very different experiments, FACS versus image analysis. FACS analysis assesses the expression of integrins on non-adherent cells therefore having access to all receptors on the cell surface. In the case of the receptor quantification via image analysis, the binding assay is performed on adherent cells and the ligand has access only to cellular receptors that are not engaged in the adhesion process, especially that the α_6 integrin binds to extracellular matrix it might be expected to yield a lower measurement.

We further sought to confirm that the trivalent construct was indeed binding via the $\alpha_6\beta_1$-integrin. We performed western blot analysis for the α_6-integrin on pull down assays using the multivalent constructs. Cell extracts were incubated with streptavidin coated beads bound with biotinylated trivalent constructs. These were analyzed by western blot for α_6-integrin. The results, Figure 6, show bands slightly below 125 kDa for the pull downs from SF767 and NHA samples (lanes 1 and 2). A negative control (lane 5), pull down minus the biotinylated construct, lacks the band near 125 kDa. A positive control sample known to contain the $\alpha_6\beta_1$-integrin (cell lysate of hepatocyte cell used as positive control by the manufacturer of the anti-α_6 antibodies, Santa Cruz) shows the same band near 125 kDa which is the expected size of the α_6-subunit. The results of the western blot demonstrate that the construct binds to the α_6-integrin. Moreover the results of the Western analysis are supportive of the ratio of increased $\alpha_6\beta_1$-integrin expression; however, Western blot analysis is not as quantitative as FACS so was not used for curve fitting.

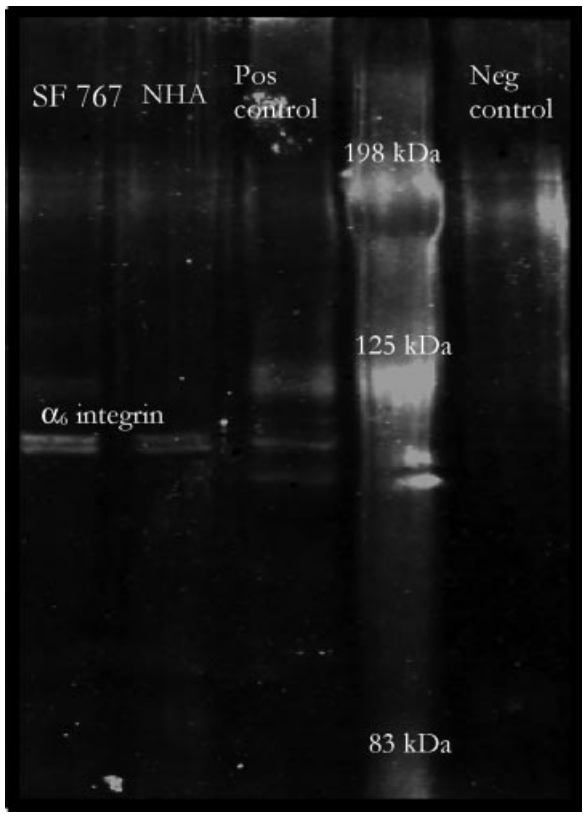

Figure 6. Western blot analysis for α_6-integrin on cell extracts pulled down using trivalent constructs. **Lanes 1** and **2** contain pull down from glioma cells and astrocyte cells respectively. **Lane 3** represents a positive control, and **lane 4** contains molecular markers. **Lane 5** is glioma cell extract pulled down using beads without trivalent construct.

Discussion

Molecular targeting via ligands or antibodies holds the potential to improve detection, localization, and treatment of cellular pathologies such as cancer. To achieve this potential, such constructs must bind in greater numbers to the pathological (target) cells than to normal (non-target) cells. We define the ratio of binding between these types of cells as *specificity*. In earlier theoretical work by two of us

(Caplan and Rosca, 2005), we predicted that specificity of multivalent constructs would be concentration dependent with specificity being equal to the ratio of receptor expression at high concentration and with specificity increasing to a maximum as concentration decreases below the receptor–ligand affinity. In contrast a monovalent construct, single peptide ligand, was predicted to exhibit specificity equal to the ratio of receptor expression at all concentrations. Here we perform experiments to determine if multivalent constructs behave as the biophysical model would predict. Successful validation would accomplish two purposes. First, it would confirm the behavior predicted which would provide an important principle for design of molecular targeting constructs. Secondly, validation would also confirm that the important biophysical phenomena are included in the model indicating that phenomena excluded from the model were in fact not important to the behavior of these constructs.

At 4°C the trend of specificity versus concentration for trivalent constructs is similar to that predicted: specificity at high concentration is near that of the receptor ratio, and specificity increases to a maximum plateau as concentration decreases. However, the quantitative aspects of the prediction are not matched exactly; the model under-predicts the concentration at which specificity transitions from low to high and the maximal value of specificity is a strong function of the fitted parameter V_R.

The concentration at which the transition from low to high affinity occurs is mostly a function of the parameter α as shown in Figure 3C. α, R_0/K_D, includes the receptor–ligand affinity (K_D) and must be two orders-of-magnitude weaker than the experimentally determined value to predict the transition concentration accurately. Above we speculated that there are two likely possibilities for this. First, incorporation of the linear peptide sequences could have decreased its affinity by two orders-of-magnitude by sterically limiting its accessibility and conformational mobility. It is also possible that decreasing the temperature to 4°C could have decreased the affinity from the experimentally measured value (measured at 37°C) by two orders-of-magnitude; but, because these authors believe this to be a less likely possibility, the affinity was not measured at 4°C. Work by Sklar et al. investigated the dynamics of ligand–receptor interaction on neutrophils. They observed changes in K_D with temperature that were within one order of magnitude (Sklar et al., 1984). From our collaborators we also have insight that the affinity is greatly affected by the linkers that are incorporated in the multivalent construct. Based on their work (Vagner et al., 2004) we observed that these changes are more dramatic in comparison to the temperature measurements; thus, this is more likely to be the main contributor to the differences observed in affinity. Second, the under-prediction of the transition concentration could indicate that the equations themselves are not including a biophysical phenomenon important to the function of these constructs. At this time these authors do not have any specific reason to believe that this is the case; however, it is a possibility.

Since there is a tradeoff between dose (or intensity) and specificity, it is critical to include the requirement for a minimum effective dose or minimum detectable intensity when designing multivalent constructs. For example, the minimum effective therapeutic concentration of doxorubicin for systemic delivery is 50 mg/kg which is approximately 90 μM. According to this study the maximum concentration for achieving an increase in specificity due to multivalency (0.6 μM) is approximately two orders-of-magnitude less than this concentration; however, 90 μM represents the systemic vascular concentration whereas 0.6 μM represents local concentration in the target tissue. Transport barriers between the vasculature and the tissue, in addition to decreasing concentration of drug in the bloodstream over time (due to kidney clearance and other metabolic processes), make the actual concentration in the target tissue 1-2% of the systemic dose (Bibby et al., 2005). Therefore, direct injection of multivalent targeting constructs to the tissue, as has been proposed by one of us previously (Stukel et al., 2008), can potentially achieve both a therapeutic concentration and specificity by injecting approximately 1 μM construct directly into the tissue. However, some patients may require a greater dose of therapeutic compound to achieve efficacy, and in that case specificity may be lost as concentration of the drug is titrated to greater concentrations. This problem can be addressed either by modifying construct design to decrease the maximum concentration at which high specificity is achieved (potentially through increasing valence, although this has not been tested in this study) or by decreasing minimum effective dose by choosing a therapeutic that has a lower minimum effective dose.

The binding enhancement factor (V_R) value that best fits the data, 1.7×10^6, results in a maximal specificity that is greater than specificity measured at the two lowest concentrations and V_R is also greater than expected. As can be seen in Figure 3C, increasing V_R makes the transition to greater specificity steeper. In our previous work we estimated V_R to be 1×10^5, and in recent work by Shewmake et al. (2008) in which V_R is fit to experimental avidity data an estimate of $V_R \sim 150$ is determined. The linkers used here are different than those studied by Shewmake as is the receptor system so it is possible that V_R values for the constructs studied here are greater. Regardless, although unexpected based on these previous estimates of V_R, the sharp transition to increased specificity is a welcome development as this suggests that reasonably high concentrations of construct can achieve levels of specificity that are likely to be useful clinically. The over-prediction of maximal specificity could also be due to non-specific binding of constructs to the substrate which would result in an experimentally measured value of specificity less than the predicted value.

The specificity achieved in these experiments, approximately 10-fold, has potential to be very useful clinically;

however, these experiments were performed at 4°C. Obviously cooling patients to 4°C prior to therapy or imaging is not viable so experiments were also performed to show the difference in behavior at 37°C. As shown in Figure 4, there is intense fluorescence in SF767 cells and NHA cells at both 10 and 0.625 μM trivalent construct; therefore, the ratio of fluorescence (specificity) is low. This fluorescence is persistent after trypsin treatment (Fig. 5) suggesting that both target and non-target cells have internalized the trivalent construct. Further evidence to support internalization is that cells similarly treated with trypsin but which bound the construct at 4°C retained little to no fluorescence. These observations run counter to conventional wisdom that internalization is a mechanism to achieve specificity by using multivalency to induce target cells to internalize the constructs. Rather we find, since constructs must be presented to both cell types at equal concentration, that non-target cells are able to internalize constructs at a similar rate as do target cells. Although the data at 4°C seem to validate the biophysical model and establish proof-of-principle for achieving targeting specificity, it seems that internalization at 37°C presents a technical hurdle to the clinical applicability of these constructs. These authors believe that this may be overcome by careful choice of receptor targets and ligand development by either choosing a receptor–ligand combination that does not internalize or a receptor–ligand combination that will internalize rapidly on the target cell but not on non-target cells. Identification of receptor targets for this type of targeting strategy is an open area of research. It has proven difficult to find single receptor targets that are over-expressed when compared to all other cell types exposed to the construct. In this work, we have chosen to target the $\alpha_6\beta_1$-integrin because (1) it is known to be over-expressed on glioma cells compared to normal astrocytes and other brain cells, (2) the number of integrins expressed is over 10,000 which is also important to enhancing specificity through multivalency (Caplan and Rosca, 2005), and (3) targeting an integrin may also have the added benefit of inhibiting glioma cell invasion. It is clear from our research here that a further constraint on receptor choice may be that it is not internalized rapidly by non-target cells. As mentioned above, the molecular targeting literature considers internalization a route to enhanced specificity rather than a hindrance to achieving specificity. The study here presents the possibility that receptor choice may dictate which effect internalization has upon specific targeting.

Conclusion

Previous theoretical work predicted that enhancement of specificity due to multivalency would only be achieved at low concentration. Here we confirm experimentally the general trend predicted when experiments are performed at 4°C. Although the transition from low to high specificity is sharper than predicted and the concentration at which this transition occurs is under-predicted, the model does capture the fact that the transition to high specificity occurs at concentration less than the receptor–ligand affinity. Experiments at 37°C reveal the importance of internalization; however, in this system internalization decreases specificity which runs counter to the conventional wisdom that multivalency will achieve specificity via internalization. Careful choice of receptor–ligand combination will be necessary to achieve clinically relevant levels of specificity under physiologic conditions.

The authors thank our funding sources: NIH (R21 NS051310, K22 DE014386), Arizona Biomedical Research Commission Grant 0606 and our collaborators Michael Berens (Translational Genomic Institute), Josef Vagner (University of Arizona), and Heather Maynard (UCLA). Recognition is given to Dr. Michael Berens, Dr. Dominique Hoelzinger, and Dr. Tim Demuth for assistance with obtaining and validating cell lines. We thank Dr. Charles Flynn for assisting with the imaging. We also thank Dr. Dan Brune and John Lopez for their generous assistance and advice with the construct synthesis.

References

Balthasar S, Michaelis K, Dinauer N, von Briesen H, Kreuter J, Langer K. 2005. Preparation and characterisation of antibody modified gelatin nanoparticles as drug carrier system for uptake in lymphocytes. Biomaterials 26(15):2723–2732.

Bibby D, Talmadge J, Dalal M, Kurz S, Chytil K, Barry S, Shand D, Steiert M. 2005. Pharmacokinetics and biodistribution of RGD-targeted doxorubicin-loaded nanoparticles in tumor-bearing mice. Int J Pharm 193(1–2):281–290.

Cai W, Rao J, Gambhir S, Chen X. 2006. How molecular imaging is speeding up antiangiogenic drug development. Mol Cancer Ther 5(11):2624–2633.

Caplan MR, Rosca EV. 2005. Targeting drugs to combinations of receptors: A modeling analysis of potential specificity. Ann Biomed Eng 33(8): 1126–1137.

Carlson C, Mowery P, Owen R, Dykhuizen E, Kiessling L. 2007. Selective tumor cell targeting using low-affinity, multivalent interactions. ACS Chem Biol 2(2):119–127.

Gaietta G, Redelmeier TE, Jackson MR, Tamura RN, Quaranta V. 1994. Quantitative measurement of alpha 6 beta 1 and alpha 6 beta 4 integrin internalization under cross-linking conditions: A possible role for alpha 6 cytoplasmic domains. J Cell Sci 107(Pt 12):3339–3349.

Gingras M-C, Roussel E, Bruner JM, Branch CD, Moser RP. 1995. Comparison of cell adhesion molecule expression between glioblastoma multiforme and autologous normal brain tissue. J Neuroimmunol 57: 143–153.

Handl HL, Vagner J, Yamamura HI, Hruby VJ, Gillies RJ. 2004. Lanthanide-based time-resolved fluorescence of in cyto ligand–receptor interactions. Anal Biochem 330(2):242–250.

Lowery A, Gobin A, Emily D, Halas J, West J. 2006. Immunonoanoshells for targeted photothermal ablation of tumor cells. Int J Nanomed 1(2): 149–154.

Madhankumar A, Slagle-Webb B, Mintz A, Sheehan J, Connor J. 2006. Interleukin-13 receptor-targeted nanovesicles are a potential therapy for glioblastoma multiforme. Mol Cancer Ther 5(12):3162–3169.

Nakahara H, Nomizu M, Akiyama SK, Yamada Y, Yeh Y, Chen W-T. 1996. A mechanism for regulation of melanoma invasion: Ligation of alpha6beta1 integrin by laminin G peptides. J Biol Chem 271(44): 27221–27224.

Rosca EV, Stukel JM, Gillies RJ, Vagner J, Caplan MR. 2007. Specificity and mobility of biomacromolecular, multivalent constructs for cellular targeting. Biomacromolecules 8(12):3830–3835.

Rosenthal E, Kulbersh B, King T, Chaudhuri T, Zinn K. 2007. Use of fluorescent labeled anti-epidermal growth factor receptor antibody to image head and neck squamous cell carcinoma xenografts. Mol Cancer Ther 6(4):1230–1238.

Shewmake TA, Solis FJ, Gillies RJ, Caplan MR. 2008. Effects of linker length and flexibility on multivalent targeting. Biomacromolecules 9(11): 3057–3064.

Sklar LA, Finney DA, Oades ZG, Jesaitis AJ, Painter RG, Cochrane CG. 1984. The dynamics of ligand-receptor interactions. Real-time analyses of association, dissociation, and internalization of an N-formyl peptide and its receptors on the human neutrophil. J Biol Chem 259(9):5661–5669.

Stukel JM, Heys JJ, Caplan MR. 2008. Optimizing delivery of multivalent targeting constructs for detection of secondary tumors. Ann Biomed Eng 36(7):1291–1304.

Vagner J, Handl HL, Gillies RJ, Hruby VJ. 2004. Novel targeting strategy based on multimeric ligands for drug delivery and molecular imaging: Homooligomers of alpha-MSH. Bioorg Med Chem Lett 14(1):211–215.

Ye Y, Bloch S, Xu B, Achilefu S. 2006. Design, synthesis, and evaluation of near infrared fluorescent multimeric RGD peptides for targeting tumors. J Med Chem 49(7):2268–2275.